

AperTO - Archivio Istituzionale Open Access dell'Università di Torino

**The use of contrast-enhanced ultrasonography for the detection of active renal hemorrhage in a dog with spontaneous kidney rupture resulting in hemoperitoneum**

**This is the author's manuscript**

*Original Citation:*

*Availability:*

This version is available <http://hdl.handle.net/2318/153725> since 2017-05-15T15:11:03Z

*Published version:*

DOI:10.1111/vec.12372

*Terms of use:*

Open Access

Anyone can freely access the full text of works made available as "Open Access". Works made available under a Creative Commons license can be used according to the terms and conditions of said license. Use of all other works requires consent of the right holder (author or publisher) if not exempted from copyright protection by the applicable law.

(Article begins on next page)

***This is an author version of the contribution published on:***

*Questa è la versione dell'autore dell'opera:*

*Journal of veterinary emergency and critical care, October 9 ,2015, DOI  
10.1111/vec.12372*

***The definitive version is available at:***

*La versione definitiva è disponibile alla URL:*

*<http://onlinelibrary.wiley.com/doi/10.1111/vec.12372/full>*

The use of contrast-enhanced ultrasonography for the detection of active renal hemorrhage in a dog with spontaneous kidney rupture resulting in hemoperitoneum

Gian Marco Gerboni, DVM; Giulia Capra, DVM; Silvia Ferro, DVM;  
Claudio Bellino, DVM, PhD; Manuela Perego, DVM; Stefania Zanet, DVM;  
Antonio D'Angelo, DVM, PhD; Paola Gianella, DVM, PhD, DACVIM

From Clinica Veterinaria Malpensa, Via Marconi 27, 21017, Samarate, Varese, Italy (Capra, Gerboni, Perego); the Department of Veterinary Sciences, University of Turin, Via L. da Vinci 44, 10095 Grugliasco, Torino, Italy (Bellino, D'Angelo, Gianella, Zanet); Department of Comparative Biomedicine and Food Science, University of Padua, Agripolis, Viale dell'Università 16, 35020 Legnaro, Padova; (Ferro).

Address correspondence and reprints request to Dr. Gianella, Department of Veterinary Sciences, University of Turin, Via L. da Vinci 44, 10095 Grugliasco, Torino, Italy.

Email: [paola.gianella@unito.it](mailto:paola.gianella@unito.it)

The authors declare no conflict of interest.

Running title: spontaneous kidney rupture in a dog

## Abstract

**Objective-**To describe the use of contrast-enhanced ultrasonography (CEUS) for the detection of active renal hemorrhage in a dog with spontaneous kidney rupture resulting in hemoperitoneum.

**Case summary-**A 9-month-old, sexually intact male Boxer dog presented for acute collapse, abdominal pain and tachycardia. Physical examination findings were consistent with hypovolemia and acute abdomen. B-mode ultrasonography revealed peritoneal effusion and a right kidney mass. Subsequently, a CEUS study was performed on the right kidney which detected active hemorrhage from that kidney resulting in both hemoretroperitoneum and hemoperitoneum. At exploratory surgery ultrasonographic findings were confirmed and a right nephrectomy was performed. Histopathology demonstrated severe parenchymal alterations along with the presence of nematode larvae. Fecal and urine testing for the presence of parasitic ova were negative. Identification of the larvae was inconclusive. At 30 days post-operatively repeat B-mode ultrasound and clinicopathologic testing was unremarkable. The dog was alive at one year post surgery with no ill effects.

**New or Unique Information Provided-**To the authors' knowledge, this is the first report of CEUS for the detection of active hemorrhage from a kidney resulting in hemoretroperitoneum and hemoperitoneum in a dog. Although rare, the finding of nematode larvae within the renal parenchyma may have been the cause of kidney rupture. Importantly, surgical removal of the kidney was curative. Benign processes causing kidney rupture such as

parasitic infestation should be considered in the working diagnosis as related to geographical location.

**Key words:** canine, contrast harmonic ultrasound, hemoperitoneum, endoparasites

CEUS Contrast-enhanced ultrasonography

## **Introduction**

Ultrasound imaging is often used in the evaluation of dogs with suspect hemoperitoneum for both diagnosis and for searching for sources of bleeding before surgery. Splenic masses are the most commonly reported source of hemorrhage in dogs with tumors, however, other abdominal organs may be involved including more commonly liver, adrenals, and kidneys with other sources possible.<sup>1-3</sup> Previous reports have shown that dogs with splenic masses and concurrent hemoperitoneum have high rates of malignancy.<sup>4</sup> There are other causes of nontraumatic hemoperitoneum including coagulopathy.<sup>2</sup> Thus, a thorough workup is imperative in deciding whether the case is medical or surgical. When a case is surgical, the detection of the source of bleeding is helpful prior to surgery in determining the degree of expertise needed for definitive stoppage of hemorrhage. Standard B-mode ultrasonography can indirectly screen for the source of hemorrhage. More advanced ultrasound techniques such as CEUS when available can in fact directly diagnose the source of bleeding. In both human and veterinary medicine, CEUS increases the sensitivity and specificity of conventional

ultrasonography and color flow Doppler, and might be a valid alternative to anesthesia and costs associated to CT or MRI.<sup>5</sup> In veterinary medicine, although the use of CEUS hold promise,<sup>6,7</sup> reports of CEUS of the kidney are still limited.<sup>8-9</sup> To the best of the authors' knowledge, the CEUS evaluation of injured renal parenchyma in a dog with spontaneous kidney rupture and subsequent hemoperitoneum has not previously been reported in the veterinary literature. In addition, the presence of nematode larvae within the renal parenchyma, which may have been cause of the kidney rupture, is discussed.

### **Case summary**

A 9-month-old, 20 kg, sexually intact male Boxer dog presented to an emergency hospital in northern Italy for evaluation of acute collapse and abdominal pain. The dog had appeared normal up until 3 hours previously when the owner observed weakness and an elevated heart rate (HR). There was no known trauma or toxin exposure. Vaccinations were current, monthly heartworm preventative therapy had been given since 2 months of age, and the prior health history was unremarkable. Abnormalities on physical examination included: pale mucous membranes, a prolonged capillary refill time, tachycardia (200 beats per minute) with weak peripheral pulses, generalized weakness, and diffuse abdominal pain on palpation. Dorsal metatarsal arterial pulses were palpable. An over-the-needle catheter was placed in the right cephalic vein and blood for a CBC, serum biochemical profile and coagulation profile was collected. A sample of urine was also submitted for dipstick evaluation and urine specific gravity assessment. A 400 ml IV bolus (20 ml/kg) of warmed lactated Ringer's solution was delivered over 15-30 minutes. Methadone<sup>a</sup> was administered at 0.1 mg/kg IM for analgesia.

Bloodwork abnormalities are shown in Table 1. A normocytic normochromic nonregenerative anemia, mature neutrophilia and thrombocytopenia were demonstrated on CBC. Prothrombin time and partial thromboplastin time were normal. Urinalysis revealed a specific gravity of 1.035 with trace hematuria on dipstick evaluation. These results were considered consistent with acute hemorrhage and subsequent decreased renal perfusion. A second sample of venous blood was collected for blood typing and the result confirmed the presence of Dog Erythrocyte Antigen (DEA) 1.1.

Ultrasonographic examination of the abdomen revealed a moderate amount of echogenic free fluid and an irregular mass approximately 6 cm X 5 cm involving the cranioventral pole of the right kidney. The majority of the mass was isoechoic to the adjacent renal cortex, with multiple internal hypoechoic foci devoid of distal acoustic enhancement (Figure 1). The ultrasonographic appearance of the remainder of the renal cortex and the corticomedullary distinction were unremarkable in the right kidney and throughout the left kidney. No other abnormalities were observed. No pleural or pericardial fluid was detected by the FAST subxiphoid view. Hemoperitoneum was diagnosed by comparative packed cell volumes of the abdominal fluid (23%) to peripheral venous blood (25%); and the finding that the abdominal sample was non-clotting. Culture of the abdominal fluid was not performed.

Based on the ultrasonographic findings, the main differential diagnoses included renal hematoma, granuloma, abscess or neoplasia associated with intra-abdominal hemorrhage. Since color flow Doppler was inconclusive, CEUS was performed in effort to determine if the kidney was actively bleeding. A total volume of 0.6 ml (0.03 ml/kg) of sulfur

hexafluoride-filled microbubbles<sup>b</sup> was injected intravenously in the right cephalic vein as a bolus, immediately followed by a 5-ml flush with sterile saline. CEUS was performed with a dedicated machine<sup>c</sup> equipped with contrast-specific imaging technology<sup>d</sup> for selective visualization of the contrast bubbles. Continuous scanning with a low mechanical index (0.07) and an acoustic pressure of 30 kPa during both early arterial and late corticomedullary phases started immediately. The early arterial phase was defined as the time during which only the arterial vessels were enhanced (5–10 seconds after injection). The late corticomedullary phase began with homogeneous enhancement of the renal cortex followed by the medulla, which gradually became isoechoic with the cortex (10 seconds to maximum 2 minutes after injection). Total recording time was 120 seconds.

Qualitative evaluation of the contrast-enhancement pattern of the right kidney revealed a large, nonvascularized mass involving its cranioventral pole. The mass was surrounded by a thin, vascularized rim in direct continuity with the adjacent isoechoic renal cortex. Both the early arterial and the late corticomedullary phases were characterized by a small area in the renal cortex without enhancement and by two hyperechoic linear to fountain-like foci with strong enhancement extending from the renal cortex into the center of the mass (Figure 2). The presence of the hyperechoic linear to fountain-like foci was considered supportive of an active renal hemorrhage causing extravasation of the contrast agent from the ruptured kidney into the center of the mass. Based on this finding an exploratory celiotomy was performed with high suspicion the source of hemorrhage was from the right kidney.

Preoperative stabilization included a transfusion of 300 ml (15 ml/kg) fresh whole blood DEA 1.1 positive in the left cephalic vein and

warmed lactated Ringer's solution at 4 ml/kg/h in the right cephalic vein. Preoperative mean arterial pressure measured by oscillometric methods<sup>c</sup> was 80 mmHg and oxygen saturation measured by pulse-oximeter<sup>c</sup> was 99% in room air during spontaneous ventilation. Approximately 200 mL of hemorrhagic fluid were removed from the abdominal cavity. Active hemorrhage was observed from an irregular mass involving the cranioventral pole of the right kidney. The remainder of the exploratory celiotomy was unremarkable with no other sources of hemorrhage being identified. A right nephrectomy was routinely performed.

The postoperative course was uncomplicated and monitoring included vital signs (temperature, pulse, respiratory rate), mean arterial pressure, urine output, and serial monitoring of cell blood count and azotemia. Injectable antibiotic therapy (enrofloxacin, 5 mg/kg, IV, q 24 h) was given postoperatively along with buprenorphine<sup>f</sup> (0.01 mg/kg IV q 8 h). The dog was weaned off IV fluids over 72 hours post-operatively and ready for patient discharge however the owner elected for the dog to stay another 3 days. The dog was prescribed enrofloxacin (5 mg/kg, PO, q 12 h) and fenbendazole (50 mg/kg, PO, q 24 h) for 2 weeks. At the time of patient discharge, 6 days post-operatively, all clinicopathological values were within the normal limits with the exception of a packed cell volume of 28%.

The right kidney was sectioned mid-sagittally. On the cut surface, the renal cortex was characterized by two hemorrhagic, dark red areas present in the cranio-dorsal and cranio-ventral pole of the kidney containing clots admixed with necrotic tissue (Figure 3). Light microscopy demonstrated extensive hemorrhagic areas mainly confined to the cortex, but multifocally also involving the medulla. At this level, the renal parenchyma was no longer recognizable and diffuse necrosis was also present. In the

remaining parenchyma, the glomerular compartment showed a diffuse global increase in mesangial matrix and focal global sclerosis associated with mild periglomerular fibrosis. Multifocal moderate podocyte hypertrophy with occasional sclerohyalinosis and rarely Bowman's capsule mineralizations were observed. Multifocal eosinophilic amorphous material was occasionally detected in the tubular lumina, and occasional tubular mineralizations were also evident. In addition, numerous multifocal pluricellular and cylindrical structures (at least 160  $\mu\text{m}$  in length and 11-12  $\mu\text{m}$  in diameter) were visible in the lumen of the glomerular capillaries (Figure 4), occasionally in the lumen of the tubuli, and rarely in the interstitium, where they were associated with a mononuclear infiltrate with giant cells. These structures were compatible with nematode larvae. Unstained slides were submitted to a diagnostic laboratory<sup>g</sup> for genetic identification.<sup>10</sup>

In an attempt to identify the nematode larvae, serial fecal tests, including direct smears, zinc sulfate flotation, and fecal Baermann, and routine urinalysis were performed. No parasite ova or larvae in either the urine or feces were detected. PCR results were negative.

On follow-up examination one-month post-operatively, B-mode abdominal ultrasound was unremarkable and no clinical pathological abnormalities were found. At one year post-operatively the dog was alive with no associated morbidity.

## **Discussion**

The case report documents the more advanced use of ultrasound using CEUS to help localize preoperatively active renal hemorrhage in a dog with spontaneous kidney rupture resulting in hemoretroperitoneum and hemoperitoneum. Interestingly, nematode larvae were found on

histopathology. The parasitic infection may not have been an incidental finding but rather could have been the cause of kidney rupture. Such a curative treatable benign process should be considered in appropriate geographical locations within the world.

B-mode ultrasonography is routinely used for indirectly evaluating for abdominal injuries and intra-abdominal bleeding through the detection of free fluid.<sup>11</sup> The focused assessment with ultrasonography for trauma (FAST) examination, by virtue of its higher specificity and sensitivity in the detection of free fluid/hemorrhage as compared with diagnostic peritoneal lavage and computed tomography, has become an increasingly common diagnostic modality in human trauma patients<sup>12</sup> and has been reported to improve patient assessment and care.<sup>13,14</sup> In human trauma patients, hemoperitoneum scoring systems based on FAST findings are utilized to semiquantitatively assess the degree of intra-abdominal hemorrhage.<sup>15</sup> In veterinary medicine, the abdominal focused assessment with ultrasonography for trauma (AFAST) examination has been applied for the detection of free abdominal fluid, other intra-abdominal pathologies, and possibly pleural and pericardial injuries in patients with and without trauma, and particularly in those with cardiovascular instability.<sup>16,17</sup>

Furthermore, because the serial AFAST examination can detect delayed fluid accumulation not apparent on initial AFAST scans, it is used in combination with an abdominal fluid score (AFS) to detect changes in the quantity of abdominal fluid over time.<sup>18</sup> By combining the AFS system with initial and serial AFAST scans, the degree of ensuing anemia in acutely hemorrhaging dogs may be anticipated and a semiquantitative measurement of free abdominal fluid obtained. This provides the clinician with a powerful tool for assessing injury severity and a more reliable means than

radiographic assessment of abdominal trauma than simply evaluating admission hematocrit and total serum protein.<sup>16,18</sup> However, there are limitations to sonographic detection and FAST examination of parenchymal injuries, especially of lower grade injuries,<sup>19,20</sup> and B-mode ultrasound examination may widen the differential diagnosis for an abnormal finding, as in the present case. To date, the AFAST examination has not been evaluated in veterinary medicine for the detection of solid organ or retroperitoneal injury after blunt abdominal trauma.<sup>17</sup> Here, AFAST was used to detect the presence of hemoperitoneum, but it could also have been further applied in combination with the AFS to semiquantitate the degree of bleeding. Also, AFAST and AFS could have been combined to postoperatively screen for the recurrence or resolution of bleeding. Indeed, human and veterinary studies have shown the clinical value of serial exams.<sup>15,16,18,21</sup>

B-mode and color flow Doppler ultrasonography provide less detailed blood flow information than either computed tomography or magnetic resonance imaging.<sup>22-24</sup> In contrast, CEUS is useful in the evaluation of vascular lesions,<sup>25</sup> vascular devices,<sup>26</sup> in distinguishing between benign and malignant focal parenchymal lesions,<sup>8</sup> and for improving the detection of active, ongoing and potentially life-threatening hemorrhages.<sup>25,27</sup> Indeed, contrast medium extravasation will appear hyperechoic to adjacent parenchyma, as in the present case, where the presence of two hyperechoic linear to fountain-like foci, not recognized with B-mode or color flow Doppler ultrasonography, was presumably due to extravasation of the contrast agent from the ruptured kidney into the large hematoma.<sup>27</sup> Although CEUS has been used to visualize blood flow extravasation in human medicine,<sup>25,27</sup> such use in veterinary patients has been reported only in experimental canine and porcine models.<sup>28,29</sup>

The most important disadvantages of CEUS include poor stability of ultrasonographic contrast agents and the need for operator expertise and specialized equipment, which increase the cost and reduce the availability of this imaging technique.<sup>30</sup> Indeed, sophisticated ultrasound machines must be equipped with Doppler modalities, special low-frequency transducers, software that permits performance of contrast-specific imaging, and, eventually, software for quantitative evaluation of CEUS images.<sup>30</sup> Another potential limitation is the time-sensitive nature of the scan; if a diagnostic scan is not acquired or a re-evaluation is necessary, further administration of the contrast agent would be required.<sup>31</sup> Moreover, in humans, some adverse effects have been reported.<sup>32</sup> In general, ultrasonographic contrast agents are well tolerated for abdominal examinations, with minor and self-resolving adverse events (eg. headache, nausea, altered taste or sensation of heat).<sup>32</sup> Generalized allergy-like reactions occur rarely.<sup>32</sup> To date, no adverse reactions have been reported in dogs.<sup>30</sup>

To the authors' knowledge, spontaneous kidney rupture as a cause of hemoperitoneum is a rare scenario in veterinary medicine,<sup>1</sup> while nematode larvae present within the renal parenchyma, as the possible cause of kidney rupture have never been reported before. Splenic, hepatic, and adrenal masses have been associated with nontraumatic hemoperitoneum in the dog,<sup>2,3</sup> with the spleen reported as the most common source of hemorrhage; however, any mass of the kidney could outgrow its blood supply and result in hemorrhage.<sup>33-35</sup> In this case, culture of hemorrhagic fluid was not performed during the initial diagnostic work up because of logistic concerns, while PCR was attempted at a later date<sup>10,g</sup> because the final histological diagnosis of nematode larvae was unexpected. The absence of DNA amplification by PCR might have been due to DNA deterioration after paraffin embedding of the specimens. Furthermore, though the

morphological features of the larvae could not be completely reconstructed, not even from serial histological sectioning, the authors may hazard a guess as to their identity. Most of the larvae were found in the glomerular capillary lumen and the periglomerular fibrosis was mild, suggesting a hematogenous route of infestation. In addition, the rare presence of interstitial granulomas does not support the hypothesis for larva migrans visceralis. Numerous larvae were present within the renal parenchyma, but no remarkable eosinophilic infiltration was noted. As eosinophils are known to play an important role in the defence against parasitic diseases, this finding was unexpected, but consistent with previous reports of nematode infestations which describe histopathological lesions without or with only a mild eosinophilic component.<sup>36</sup>

With regard to the possible involved nematodes, a list with pertinent information is depicted in Table 2.<sup>36-42</sup> *Dioctophyma renale* larvae could not be excluded, even if the absence of reports of this nematode infection in Italy make this hypothesis unlikely. Based on the preventative therapy, diameter of the larvae, tissue distribution and/or little pathogenic significance in dogs, filarial parasites infection was considered unlikely as well. To the contrary, *Angiostrongylus vasorum* infection was considered likely based on the hematogenous route of dissemination, the similarity of histological lesions and the presence of hemorrhage. Indeed, coagulopathies represent a common reported manifestation of this infection,<sup>36</sup> even though the severity of bleeding correlates poorly with the extent of detectable coagulation abnormalities.<sup>39</sup> The exact pathophysiologic mechanism for the coagulation derangements is not understood; it may be that endothelial disruption by the migrating larvae and adult parasites could result in DIC.<sup>39</sup> However, because the PCR results were negative, a definitive confirmation of angiostrongylosis could not be made and remains speculative at best.

With regard to the kidney rupture and subsequent hematoma formation, it is authors' opinion that the presence of the numerous worms in the renal parenchyma could have played a role. Although uncommonly reported, another nematode that can cause kidney rupture is *Dioctophyma renale*.<sup>40</sup> Other additional hemostasis disorders, such as DIC with consumptive thrombocytopenia, immune-mediated thrombocytopenia or von Willebrand factor deficiency should also be considered.<sup>38,42</sup>

The severe thrombocytopenia observed here could be merely a consequence of acute hemorrhage; however, since disorders of consumption generally result in a mild or moderate degree of thrombocytopenia,<sup>43</sup> a combined defect such as hemorrhage and DIC or a concomitant immune-mediated destruction could not be excluded. In this case, however, the presence of an eventually adjunctive hemostasis disorder was not investigated and it was ruled out by the dog having a full recovery with no morbidity at one year post-operatively.

In summary, the use of CEUS when available may be advantageously used for the direct detection of active hemorrhage over standard B-mode ultrasonography. Although technically challenging and limited in availability because of specialized equipment, CEUS should be considered as an imaging modality for dogs with hemoretroperitoneum and hemoperitoneum. Furthermore, because nematode larvae were found within the ruptured kidney parenchyma, benign curable conditions should be considered in the differential diagnosis of such cases.

### **Footnotes**

a Semfortan, 10 mg/ml, ATI, Ozzano Emilia, Bologna

b Sonovue, Bracco Diagnostic Inc., Milan, Italy.

c MyLab 30VET, microconvex array 6.6-8 MHz, Esaote, Genoa, Italy.

d Contrast tuned imaging, convex array 5 MHz, 10 cm depth, Esaote.

e Philips M3046A

f Temgesic, 0.3 mg/ml, RB Pharmaceuticals Limited, Berkshire, United Kingdom

g Parasitology Laboratory, Department of Veterinary Sciences, Via L. da Vinci 44, 10095, Grugliasco (To), Italy

## References

1. Locke JE, Barber LG. Comparative aspects and clinical outcomes of canine renal hemangiosarcoma. *J Vet Intern Med* 2006; 20(4):962-967
2. Pintar J, Breitschwerdt EB, Hardie EM, Spaulding KA. Acute nontraumatic hemoabdomen in the dog: a retrospective analysis of 39 cases (1987-2001). *J Am Anim Hosp Assoc* 2003; 39(6):518-522
3. Aronsohn MG, Dubiel B, Roberts B, Powers BE. Prognosis for nontraumatic hemoperitoneum in the dog: a retrospective analysis of 60 cases (2003-2006). *J Am Anim Hosp Assoc* 2009; 45(2):72-77
4. Lux CN, Culp WT, Mayhew PD, et al. Perioperative outcome in dogs with hemoperitoneum: 83 cases (2005-2010). *J Am Vet Med Assoc* 2013; 242(10):1385-1391
5. Cantisani V, Ricci P, Grazhdani H, et al. Prospective comparative analysis of colour-doppler ultrasound, contrast-enhanced ultrasound, computed

- tomography and magnetic resonance in detecting endoleak after endovascular abdominal aortic aneurysm repair. *Eur J Vasc Endovasc Surg* 2011; 41(2): 186-192
6. O'Brien RT. Improved detection of metastatic hepatic hemangiosarcoma nodules with contrast ultrasound in three dogs. *Vet Radiol Ultrasound* 2007; 48(2):146-148
7. Ivancic M, Long F, Seiler GS. Contrast harmonic ultrasonography of splenic masses and associated liver nodules in dogs. *J Am Vet Med Assoc* 2009; 234(1):88-94
8. Haers H, Vignoli M, Paes G, et al. Contrast harmonic ultrasonographic appearance of focal space-occupying renal lesions. *Vet Radiol Ultrasound* 2010; 51(5):516-522
9. Haers H, Smets P, Pey P, et al. Contrast harmonic ultrasound appearance of consecutive percutaneous renal biopsies in dogs. *Vet Radiol Ultrasound* 2011; 52(6):640-7
10. Powers TO, Neher DA, Mullin P, et al. Tropical nematode diversity: vertical stratification of nematode communities in a Costa Rican humid lowland rainforest. *Mol Ecol* 2009; 18(5):985-996
11. Ara R, Khan N, Chakraborty RK et al, Ultrasound evaluation of traumatic patient in a tertiary level hospital. *Mymensingh Med J* 2013 22(2): 255-60
12. Boulanger BR, McLellan BA, Brenneman FD, et al. Emergent abdominal sonography as a screening test in a new diagnostic algorithm for blunt trauma. *J Trauma* 1996; 40(6):867-874

13. Bilello JF, David JW, Lemaster D, et al. Prehospital hypotension in blunt trauma: identifying the “crump factor”. *J Trauma* 2011; 70(5): 1038-1042
14. Ollerton JE, Sugrue M, Balogh Z, et al. Prospective study to evaluate the influence of FAST on trauma patient management. *J Trauma* 2006; 60(4): 785-791
15. McKenney KL, McKenney MG, Cohn SM, et al. Hemoperitoneum score helps determine need for therapeutic laparotomy. *J Trauma* 2001; 50(4):650–656)
16. Lisciandro GR. Abdominal and thoracic focused assessment with sonography for trauma, triage, and monitoring in small animals. *J Vet Emerg Crit Care* 2011; 21(2):104-122
17. Boysen SR, Lisciandro GR. The use of ultrasound for dogs and cats in the emergency room. *Vet Clin Small Anim* 2013; 43: 773-797
18. Lisciandro GR, Lagutchick MS, Mann KA, et al. Evaluation of an abdominal fluid scoring system determined using abdominal focused assessment with sonography for trauma in 101 dogs with motor vehicle trauma. *J Vet Emerg Crit Care* 2009; 21 (2): 104-122
19. Rozycki GS, Knudson MM, Shackford SR, Dicker R. Surgeon-performed bedside organ assessment with sonography after trauma (BOAST): a pilot study from the WTA multicenter group. *J Trauma* 2005; 59: 1356-1364
20. Poletti PA, Kinkel K, Vermeulen B, et al. Blunt abdominal trauma: should US be used to detect both free fluid and organ injuries? *Radiology* 2003; 227(1): 95-103

21. Blackbourne LH, Soffer D, McKenney M, et al. Secondary ultrasound examination increases the sensitivity of the FAST exam in blunt trauma. *J Trauma* 20014; 57(5): 934-938
22. Mortelet KJ, Cantisani V, Brown DL, Ros PR. Spontaneous intraperitoneal hemorrhage: imaging features. *Radiol Clin North Am* 2003; 41(6):1183-1201
23. Shanaman MM, Schwarz T, Gal A, O'Brien RT. Comparison between survey radiography, B-mode ultrasonography, contrast-enhanced ultrasonography and contrast-enhanced multi-detector computed tomography findings in dogs with acute abdominal signs. *Vet Radiol Ultrasound* 2013; August 6. Epub ahead of print
24. Beissert M, Delorme S, Mutze S, et al. Comparison of B-mode and conventional colour/power Doppler ultrasound, contrast-enhanced Doppler ultrasound and spiral CT in the diagnosis of focal lesions of the liver: Results of a multicentre study. *Ultraschall Med* 2002, 23(4):245-250
25. Luo W, Zderic V, Carter S, et al. Detection of bleeding in injured femoral arteries with contrast-enhanced sonography. *J Ultrasound Med* 2006; 25(9):1169–1177
26. Baglini R, Amaducci A, D'Ancona G. Left main coronary in-stent intimal hyperplasia and hemodynamics as detected by contrast-enhanced transesophageal echocardiography. *Echocardiography* 2013, 30(3): 317-323
27. Catalano O, Cusati B, Nunziata A, Siani A. Active abdominal bleeding: contrast-enhanced sonography. *Abdom Imaging* 2006; 31(1):9-16
28. Schmiedt UP, Carter S, Marin RW, et al. Sonographic detection of acute parenchymal injury in an experimental porcine model of renal hemorrhage:

- gray-scale imaging using a sonographic contrast agent. *Am J Roentgenol* 1999; 173(5): 1289-1294
29. Goldberg BB, Merton DA, Liu JB, Forsberg F. Evaluation of bleeding sites with a tissue-specific sonographic contrast-agent: preliminary experiences in an animal model. *J Ultrasound Med* 1988; 17:609-616
30. Haers H, Saunders JH Review of clinical characteristics and applications of contrast-enhanced ultrasonography in dogs. *J Am Vet Med Assoc* 2009;234(4):460–470
31. Badea R, Ciobanu L. Contrast enhanced and Doppler ultrasonography in the characterization of the microcirculation. Expectancies and performances. *Med Ultrason* 2012, 14(4): 307-317
32. Jacobsen JA, Oyen R, Thomsen HS, et al. Safety of ultrasound contrast agents. *Eur Radiol* 2005; 15 (5): 941-945
33. Bryan JN, Henry CJ, Turnquist SE, et al. Primary renal neoplasia of dogs. *J Vet Intern Med* 2006; 20(5): 1155-1160
34. Robison RL, Grosenstein PA, Argentieri GJ. Mixed mesenchymal tumor in the kidney of a young beagle dog. *Toxicol Pathol* 1997; 25(3): 326-328
35. Eddlestone S, Taboada J, Senior D, Paulsen DB. Renal haemangioma in a dog. *J Small Anim Pract* 1999; 40(3): 132-135
36. Chapman PS, Boag AK, Guitian J, Boswood A. Angiostrongylus vasorum infection in 23 dogs (1999–2002). *J Small Anim Pract* 2004; 45:435–440
37. Taylor MA, Coop RL, Wall RL. Parasites of dogs and cats. In: Taylor MA, Coop RL, Wall RL, editors. *Veterinary Parasitology*. 3rd ed. Blackwell Publishing; 2007, pp. 410, 434-435

38. Whitley NT, Corzo-Menendez N, Carmichael NG, McGarry JW. Cerebral and conjunctival haemorrhages associated with von Willebrand factor deficiency and canine angiostrongylosis. *J Small Anim Pract* 2005; 46(2): 75–78
39. Helm JR, Morgan ER, Jackson MW, Wotton P, Bell R. Canine angiostrongylosis: an emerging disease in Europe. *J Vet Emerg Crit Care* 2010; 20(1): 98-109
40. GB Wislocki. Observations on *Diocotophyme renale* in dogs. *The journal of parasitology* 1919; 6(2): 94-97
41. Otranto D, Dantas-Torres F, Brianti E, et al. Vector-borne helminths in dogs and humans in Europe. *Parasit Vectors* 2013; 16(6): 1-14
42. Garosi LS, Platt SR, McConnell JF, et al. Intracranial haemorrhage associated with *Angiostrongylus vasorum* infection in three dogs. *J Small Anim Pract* 2005 46(2): 93–99
43. Hackner SG. Bleeding disorders. In: Silverstein DC, Hopper K, editors. *Small animal critical care medicine*. 1<sup>st</sup> ed. Saunders Elsevier; 2009, pp. 507-514

### **Figure Legends**

Figure 1. Ultrasonographic longitudinal view of the right kidney. Note the mass (white arrowheads) mildly heterogeneous with the majority of it being isoechoic to the adjacent renal cortex (black arrows), but having multiple internal hypoechoic foci devoid of distal acoustic enhancement.

Microconvex array, 6.6 MHz, 9 cm depth.

Figure 2. Early arterial phase of CEUS study. Note the two hyperechoic linear to fountain-like foci (arrow) with strong enhancement extending from the renal cortex into the center of the mass (arrowheads). Convex array, 5 MHz, 10 cm depth.

Figure 3. Mid-sagittally section of the right kidney. A large subcapsular hematoma is visible on the cranial pole of the kidney (arrowheads). Note the two hemorrhagic foci originating from the cortex (arrows).

Figure 4. Two portions of a larva are visible inside a glomerulus (arrows).  
H&E stain; bar=10  $\mu$ m.

Table 1. Abnormalities on complete blood count (CBC) and serum biochemistry panel at presentation.

Variable (reference range)	Patient Values
Hct (0.37-0.55 L/L [37-55%])	0.25 [25.2]
Hemoglobin (120-180 g/L [12-18 g/dL])	82 [8.2]
RBC (5.5 to 7.9 X 10 <sup>12</sup> cells/L [5.5 to 7.9 X 10 <sup>6</sup> cells/ $\mu$ L])	3.84 [3.84]
WBC (6.00 to 17.00 X 10 <sup>9</sup> cells/L [6,000 to 17,000/ $\mu$ L])	27.20 [27,200]
Neutrophils (3.00 to 11.50 X 10 <sup>9</sup> cells/L [3,000 to 11,500/ $\mu$ L])	22.90 [22,900]
Platelets (120 to 350 X 10 <sup>9</sup> cells/L [120 to 350 X 10 <sup>3</sup> cells/ $\mu$ L])	45 [45]
TP (55 to 77 g/L [5.5 to 7.7 g/dL])	52 [5.2]
Albumin (25 to 40 g/dL [2.5 to 4.0 g/dL])	22 [2.2]
Creatinine (35.4 to 106.1 $\mu$ mol/L [0.4 to 1.2 mg/dL])	229.8 [2.6]
BUN (1.8 to 10.7 mmol/L [5 to 30 mg/dL ])	23.9 [66.8]
Phosphorus (0.7 to 2.1 mmol/L [2.3 to 6.6 mg/dL])	2.3 [7.02]
Fibrinogen (7.3 to 17.6 $\mu$ mol/L [250 to 600 mg/dL])	3.2 [110 ]

Htc, hematocrit; RBC, red blood cells; WBC, white blood cells; TP, total protein; BUN, blood urea nitrogen

Table 2. Information regarding possible involved nematode species

Nematode species	<i>Dioctophyma renale</i> <sup>37,40</sup>	<i>Dirofilaria immitis</i> <sup>37,41</sup>	<i>Dirofilaria repens</i> <sup>37,41</sup>	<i>Dipetalonema reconditum</i> <sup>37,41</sup>	<i>Angiostrongylus vasorum</i> <sup>36-39,42</sup>
Diameter (larvae)	NA	6.8 µm	11-12 µm	4.7-5.8 µm	0.8-12 µm
Route of infection	ingestion of infected raw fish, frog or water	bloodsucking culicids mosquitoes	bloodsucking culicids mosquitoes	infected fleas, ticks, lice	ingestion of infected snail, slug or frog
Preferred tissue localization	peritoneal cavity, right kidney	pulmonary arteries, right ventricle of the heart	subcutaneous or intermuscular tissue	subcutaneous or perirenal tissue, body cavities	pulmonary arteries, right ventricle of the heart
Ectopic infections	-	occasionally glomerular capillaries and medullary vessels	-	-	nervous system, eye, liver, spleen, kidney
Miscellaneous	-	asymptomatic disease or absence of microfilaremia possible	asymptomatic disease or absence of microfilaremia possible	asymptomatic disease or absence of microfilaremia possible	asymptomatic disease, acute bleeding, false negative fecal Baermann test possible
Geographical locations	worldwide	worldwide (mostly tropical, subtropical and warm temperate regions)	Europe, Africa, Asia (mostly tropical and subtropical regions)	worldwide (most prevalent filaroid species infecting dogs in many geographical areas of the Mediterranean Basin, Middle East, South Africa, South America and Oceania)	Europe, Panama State, Brazil, Columbia, United States, Newfoundland, Australia, Uganda

NA not available

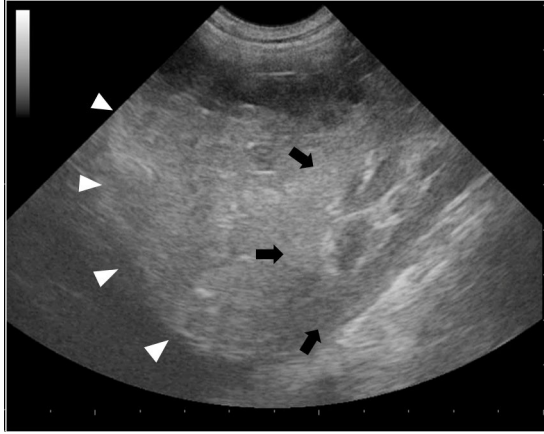


Figure 1

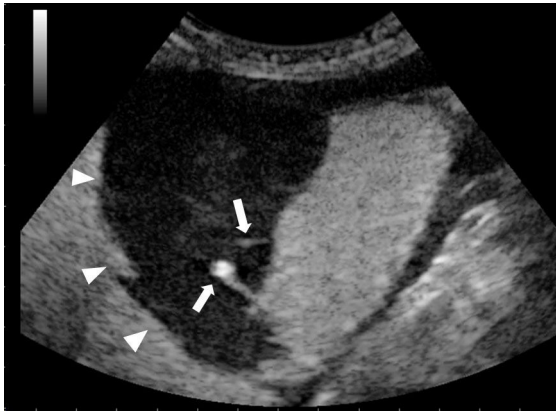
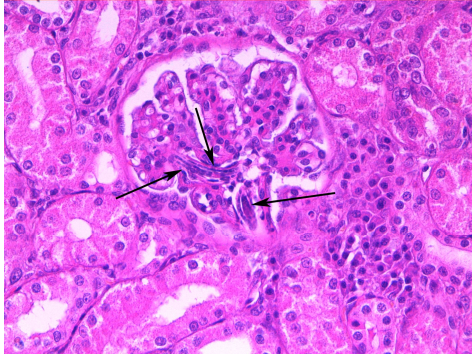


Figure 2



Figure 3



**Figure 4**